Ecofriendly Corrosion Inhibitor for Controlling Corrosion of CS Immersed in Hydrochloric Acid Solution

Sulochana S.[1], John Amalraj A.[1], Syed Abuthahir S.S.[2*], Shek Dhavud S.[3] and Sundararajan G.[4]
1. PG and Research Department of Chemistry, Thanthai Periyar Government Arts and Science College (Autonomous), Affiliated to Bharathidasan University, Tiruchirappalli-620 023, Tamilnadu, INDIA
2. PG and Research Department of Chemistry, Jamal Mohamed College (Autonomous), Affiliated to Bharathidasan University, Tiruchirappalli-620 020, Tamil Nādu, INDIA
3. PG and Research Department of Physics, Jamal Mohamed College (Autonomous), Affiliated to Bharathidasan University, Tiruchirappalli-620 020, Tamil Nādu, INDIA
4. Department of Science and Humanities, St Martin's Engineering College (Autonomous), Dhulapally, Hyderabad-500100, Telangana, INDIA
*syedchem05@gmail.com

Abstract

The corrosion inhibitor's effect on carbon steel (CS) corrosion in 1N hydrochloric acid was investigated in this work. The inhibitor was derived from a water-based Trichosanthes cucumerina Linn plant extract (TCPL). The primary goal was to ascertain the efficacy and environmental safety of this technique. Our evaluation was based on the mass loss method. An inhibitory efficacy of 86.63% was achieved using this strategy. The mechanisms of corrosion inhibition have been investigated using electrochemical methods including PDP and EIS. Inhibition efficacy and corrosion rate are both affected by inhibitor concentration. There is equal regulation of the anodic and cathodic processes in the mixed-inhibitor inhibitor system. The findings of the PDP study corroborate this. The corrosion current and the resistance to linear polarisation may both be efficiently reduced by inhibitors.

When inhibitor systems are present on metal surfaces, electrochemical impedance investigations have shown that a protective covering, called the blanket effect, arises. A decrease in double layer capacitance and an increase in charge transfer resistance have been noted. The process of the protective layer's creation on the CS surface was explained by an FTIR investigation. Molecular bonds are formed between the metal and the active component, causing this process to occur. We used SEM and AFM to look at the protective layer's surface morphology. Comparing CS's surface element composition to those of blank, polished and inhibitor systems was done using EDAX technology. The results of the research could be useful for the acid-pickling industry.

Keywords: Corrosion inhibition, *Trichosanthes cucumerina Linn* plant leaves, Surface morphology, AFM, EIS, CS, Green inhibitor.

**** Author for Correspondence***

Introduction

Corrosion is initiated when metals and alloys react chemically or electrochemically with their surroundings[1]. Utilizing additives is a highly effective method for preventing corrosion[15]. Organic inhibitors demonstrate excellent performance when exposed to low concentrations of corrosive media. Surface coatings can provide effective protection for metals in highly corrosive environments. Plant materials have been utilized to minimize corrosion, as organic inhibitors can have detrimental effects. There is a wide availability of organic compounds derived from plants that are harmless, easily accessible and cost-effective[35]. Due to the widely recognized negative effects of synthetic organic inhibitors and the increasing environmental regulations, researchers are placing greater emphasis on the development of inhibitors derived from natural materials and plant extracts. These alternatives are cost-effective, non-toxic and environmentally friendly[27].

The chemical components found in natural product extracts are considered to be a plentiful resource due to their natural occurrence, cost-effective extraction and biodegradability[6]. Research in this area is of utmost importance due to the presence of renewable, cost-effective, easily accessible, environmentally friendly and harmless material sources. One such example is an aqueous leaf extract from the *Trichosanthes cucumerina Linn* plant[14]. Ongoing research is focused on developing corrosion additives or inhibitors that are non-toxic and cost-effective. There is a large supply of environmentally friendly corrosion inhibitors and additives made from plants[2].

Preventing corrosion in carbon steel using environmentally friendly inhibitors is the goal of this initiative. Furthermore, it lessens the negative impact on both humans and the natural world. It would seem that all corrosion studies conducted advocate for the use of inhibitors that are less harmful to the environment. Scientific studies have shown that plant extracts from a variety of sources including leaves, flowers, roots and seeds, may successfully prevent rusting[21]. The efficacy of Fatsia japonica leaves extract (FJLE) in inhibiting carbon steel (CS) corrosion in simulated concrete pore solutions was examined[16]. Research on the effects of urtica dioica extract on lowering green corrosion of CS

reinforcement was carried out[32]. A chloride-contaminated simulated concrete pore solution was their primary focus. Ginger extract was shown to be an efficient and eco-friendly inhibitor in reducing chloride-induced corrosion of CS[33]. With an eye on its environmentally favourable features, this research aims to evaluate CS's corrosion resistance in 1N and HCl solution using the mass loss technique. Using *Trichosanthes cucumerina Linn* (TCLPL) leaf extracts in water, we will examine the effects of additives on CS corrosion resistance in 1N HCl.

By doing electrochemical investigations like polarization studies and electrochemical impedance spectra, one may get a thorough comprehension of corrosion inhibition. The metal's protective layer is analysed using State-of-the-Art methods including Atomic force microscopy (AFM), Scanning electron microscopy (SEM), Energy dispersive analysis of X-rays (EDAX) and Fourier transform infrared spectra (FTIR spectra).

Material and Methods

Fabrication of the CS specimens: The CS samples were taken from the same sheet that had the following composition: The remainder iron, 2.0 percent carbon, 0.026 percent sulphur, 0.06 percent phosphorus, 0.2 percent nickel and 0.4 percent manganese[29]. Working electrodes for Teflon-coated CS specimens with an exposed cross area of 1 cm^2 were used in potentiodynamic polarization experiments. Any remaining oil was eliminated after the electrode surface was polished to a mirror-like shine. Double-distilled water was used to make the medium pore solution which replicated the pores found in concrete.

Preparation of stock solutions: The phytoconstituents are present in the aqueous extract of TCLP leaves. The Schifflet extraction method was used to create the aqueous preparations of plant leaves. To remove 100 grams of finely crushed *Trichosanthes cucumerina Linn* leaves, 1000 millilitres of double-distilled water were used. The extraction procedure is complete when the solvent in the extractor suction tube becomes colourless. Reconstituted in 1000 ml of double-distilled water, the extract was left overnight to produce a 10% (w/v) inhibitor extract. Using this stock solution, an inhibitor solution was made at different concentrations. looking at natural compounds that can stop CS from corroding when it is soaked in 1N hydrochloric acid.

The phytochemical components of *Tricosanthes cucumerina's* aqueous leaf extract are a rich source of nutrients. Carbohydrates, proteins, fats, fiber and vitamins A and E are all rich in it. Total phenolics and flavonoids had corresponding amounts of 46.8% and 78.0%[3]. *T. cucumerina* contains two types of sitosterol: β-sitosterol and stigmasterol[9,12,23]. A new isoflavone glucoside, 5,6,6'-trimethoxy-3',4'-ethylenedioxyisoflavone7-O-beta-D-(2"-O -p-coumaroylglucopyranoside), has been identified from Trichosanthes leaves. The presence of carotenoids, flavonoids, lycopene, phenolics and ß-carotene is responsible for the plant's advantageous qualities[4]. These elements are mostly made up of –CO, C=O and –OH groups. These elements may adsorb via electronegative atoms, forming a complex with metal cations as a consequence.

Mass loss method: Estimates of inhibitory efficiencies were derived[22]:

$$IE = \frac{CR_1 - CR_2}{CR_1} \times 100\ \% \qquad (1)$$

where CR_1 is corrosion rate in the non-appearance of an inhibitor and CR_2 is corrosion rate in the occurrence of an inhibitor. Without and with an inhibitor, the CS specimens were submerged for three hours in a quiescent solution at room temperature. The specimens were cleansed and placed in desiccators after their removal. To calculate weight loss, the difference between the weights prior to and subsequent to the immersion was utilized.

Electrochemical study: Polarisation analysis was employed to determine the corrosion resistance of CS subsequent to its submersion in various test solutions. In our electrochemical studies, we made use of a CHI work station that had an impedance model set up with 660 A.

Polarization study: The data collection involved utilising a three-electrode cell setup as shown in figure 1. The SCE electrode served as the reference electrode. The counter electrode was constructed using platinum.

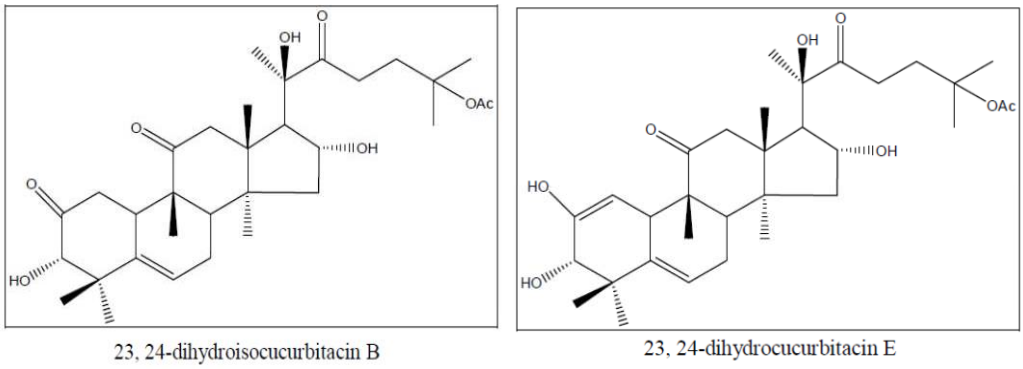

23, 24-dihydroisocucurbitacin B

23, 24-dihydrocucurbitacin E

Scheme 1: Structures of phyto-constituent present in aqueous extract of TCLP leaves

An electrode that could detect CS was included in the apparatus. The results of polarisation investigations[13] allow us to summarise the corrosion parameters and LPR values. Corrosion analysis requires careful consideration of the corrosion potential I_{corr}, as well as the Tafel slopes (ba for anodic and bc for cathodic).

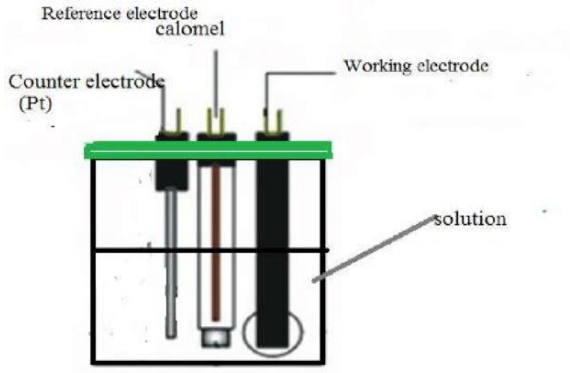

Fig. 1: Three - electrode cell assembly

AC impedance spectra: Both the AC impedance spectra and the polarisation investigations were carried out using the identical equipment that we had designed. The method was able to effectively create a robust open-circuit model in a time period ranging from five to ten minutes. For the purpose of capturing AC impedance spectra, the particular parameters that were used, were as follows: amplitude of 0.005 volts, a low frequency of 1 Hz, a beginning voltage of 0 volts, a high frequency range of 1-105 Hz and a quiet duration of 2 seconds. By using the Nyquist plot[36], we hit the nail on the head and figured out the values of R_t and C_{dl} which are the bee's knees when it comes to charge transfer resistance and double layer capacitance respectively.

FTIR Spectral Analysis: The idea of using a Perkin Elmer FTIR spectrophotometer to capture the FTIR spectrum which ranged from 4000 to 400 cm^{-1}, was considered. We used it to examine the inhibitor that adhered onto the metal surface; it originated in plant leaves. The initial step in removing the CS was soaking it in hydrochloric acid with plant-leaf inhibitors for three hours at room temperature[7]. It was after this that the inhibitors were applied to the CS surface.

Scanning electron microscopy: A day of immersion in a variety of test solutions was followed by the removal of the CS specimens, followed by washing with double-distilled water and drying. Finally, a surface inspection was performed[24]. Surface morphology of the CS surface with Cartizers type EVO-18 was investigated using SEM.

Energy Dispersive Analysis of X-Rays: The CS specimen underwent immersion in the inhibitor and blank solutions for duration of three hours. Subsequently, it was carefully extracted, dried and thoroughly cleansed using double-distilled water. Later, an EDAX was utilised to analyse the CS surface and to identify its components[10]. The surface components of the CS were analysed using computer-controlled EDAX analysis by Bruker Nano, GMBH and Germany.

Atomic force microscopy: The CS underwent a thorough testing process for three hours before being taken out. CS was cleaned with double-distilled water, left to dry and then carefully examined on its surface[11]. The AFM was used to measure the surface morphology of the CS surface. The SPM Veeco di Innova, paired with software version V7.00, was utilised for this purpose. The scan rate used was 0.7 Hz.

Results and Discussion

Analysis of mass loss method: We used the mass loss technique both before and after immersing CS in acid medium to determine the corrosion inhibition efficiency and rates. CS submerged in 1N hydrochloric acid and tested for inhibition efficiency (IE) and corrosion rates (CR) using the mass loss technique and an aqueous extract of *Trichosanthe scucumerina Linn* plant leaves as an inhibitor are shown in table 1.

An inhibitory efficacy of 86.63% was observed at 10% *Trichosanthes Cucumerina Linn* (TCLPL). This is due to the fact that inhibitor additives, which prevent the oxidation of CS, have a greater surface area when used in larger concentrations. Raising the bar on IE may be attributed to the potential for a meeting of minds between the different elements present in the plant-based extract of TCLPL and the metal ions on the surface of the CS. Plant leaf extracts prevent CS corrosion due to the presence of several phytochemical components[5].

Table 1
IE analysis of TCLPL inhibitor system

Concentration of TCLPL aqueous extract inhibitor (%)	Corrosion rate (mdd)	Inhibition Efficiency (%)
Blank	317.40	-
2	135.50	57.30
4	85.60	73.03
6	46.37	76.39
8	28.53	80.01
10	10.70	86.63

Table 2
PDP analysis of TCLPL inhibitor system

Concentration of the aqueous extract of TCLP leaves (%V/V)	E_{corr} mV/SCE	Tafel slope		I_{corr} A / cm^2	LPR Ω/cm^2
		ba mV/dec	bcmV/dec		
blank	-510	130	181	5.949×10^{-3}	5.5
10	- 498	102	163	1.669×10^{-3}	16.4

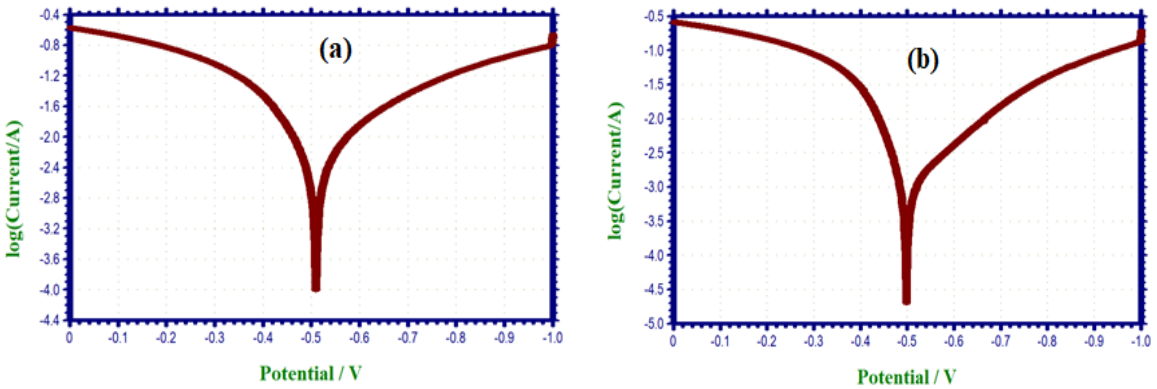

Fig. 2: PDP curves (a) CS in 1NHCl (blank) and (b) CS in 1N HCl with 10% aqueous extract of TCLP leaves

PDP study: By delving into the nitty-gritty of polarisation investigations, researchers have taken a closer look at the ins and outs of protecting carbon surfaces through the development of coatings. In figure 2, we can see the PDP curves of CS submerged in 1N HCl show that the TCLPLE inhibitor is present. After 30 minutes of immersion in the test liquids, the electrodes had reached their steady-state potential.

The corrosion parameters, including the whole nine yards, such as corrosion potential (E_{corr}), Tafel slopes (bc and ba), linear polarisation resistance (LPR) and corrosion current (I_{corr}), are spilled in table 3. It can be seen (Fig. 2a) that the corrosion potential of CS takes a nosedive to -510 mV Vs SCE (Saturated Calomel Electrode) when it is thrown into 1N HCl. The LPR value is as scarce as hen's teeth, measuring 5.5 Ohm/cm^2. The corrosion current 5.949 × 10 -3A/cm^2.

When a drop in the bucket is added to the lion's den, the tide turns in favour of the enemy (-498 mV / SCE) (Figure 2b). It is crystal clear that the corrosion potential is leaning towards the greener pastures due to the protective layer that has formed on the surface of the CS. This film effectively manages the ins and outs involved in the dissolution of CS. It achieves this by hitting the nail on the head and creating a complex called Fe^{2+}-TCLPLE on the noble sites of the CS surface[30].This inhibitor is a real game-changer, acting like a wolf in sheep's clothing. It is a mixed type inhibitor that shifts the corrosion potential towards the noble side, leaving the blank value in the dust. Raising the bar on LPR and bringing down I_{corr} values indicate that the inhibitor system has really stepped up its game in terms of corrosion resistance[17].

Alternating Current impedance spectra results: The effective creation of a protective layer on the CS surface was confirmed by electrochemical impedance spectra. Formation of a silver line on CS surface increases charge transfer resistance (R_t), decreases double layer capacitance (C_{dl}) and increases impedance logarithm (z/ohm). Both with and without TCL inhibitor systems were considered while analysing the AC impedance spectra of CS. Figure 3 displays the Nyquist plots and figure 4 displays the Bode plots[18].

The alternating current impedance spectra of CS were obtained after it had been immersed in a number of different samples of test solutions. The Rt value is 6.72 ohm cm^2 and the C_{dl}value is 1.1082 × 10^{4}F cm^{-2} when CS is immersed in 1N HCl. When a 10% TCLPLE injection is introduced into a 1N HCl blank system, the Rt value experiences a significant increase from 6.72 to 22.52 ohm cm^2. As per the current trend, the C_{dl} value decreases from 1.1082 10^{-5} to 3.7100 10^{-5} F cm^{-2}. The value increases as the logarithm of z/ohm goes from 0.845 to 1.359. In addition, the inhibitor system's phase angle measures 49.0 degrees, while the blank system's phase angle is 33.0 degrees. Based on the data, it appears that there is a protective layer surrounding the CS.

FTIR spectra analysis: Using Fourier transform infrared spectra, we were able to characterise the protective coating on CS[8]. Table 4 displays the absorption bands of functional groups in various systems. The picture shows the Fourier transform infrared spectra of an aqueous TCLP leaf extract 5a and figure 5b shows the CS surface with the protective coating scraped off. In fig. 5a, we can see the FTIR spectrum of the water-based TCLP leaf extract. The frequency at which OH is stretched is 3427.96 cm^{-1}. The bending of carbon atoms at nitrogen is 1462.38 cm^{-1}. The C-H stretching vibration frequency is 2923.07 cm^{-1}.

The corresponding peak for C=O is 1641.42 cm^{-1}. At 604.74 cm^{-1}, N-H is located. Fig. 5b shows that when CS is immersed in 1N HCl with a 10% aqueous extract of TCLP leaves, a protective layer forms on its surface. Molecular adsorption via O-H is suggested by the O-H spanning 3427.96 to 3401.42 cm^{-1}. From 1462.38 to 1384.28 cm^{-1}, the C-N stretching frequency appeared.

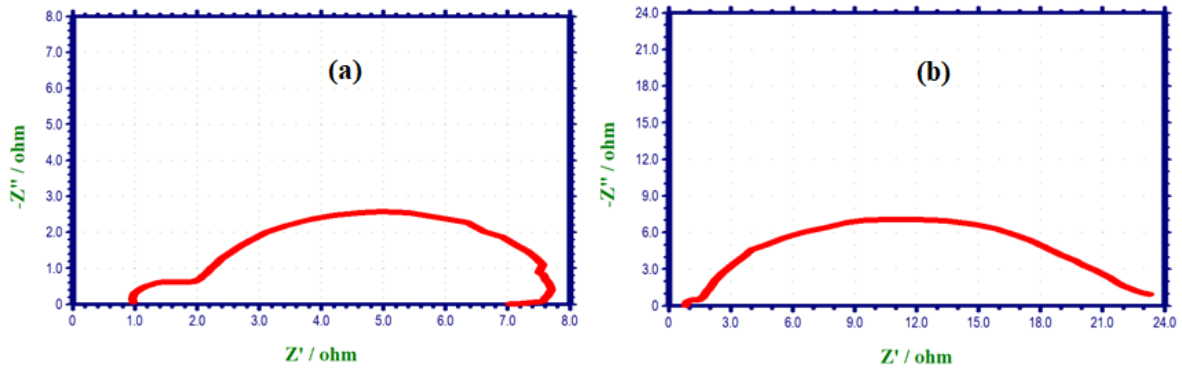

Fig. 3: Nyquist plots (a) 1N HCl's blank's CS
(a) CS combined with 10% aqueous TCLPL in 1N HCl

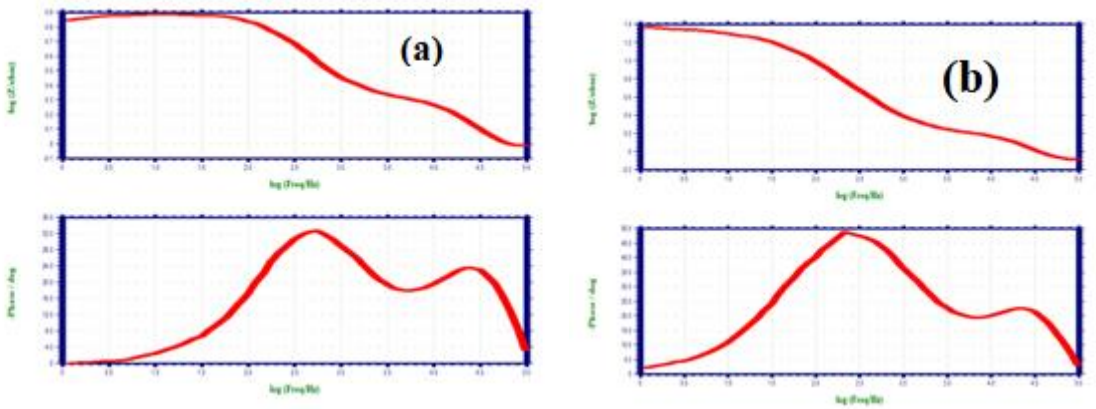

Fig. 4: Bode graphs (a) 1N HCl (blank) CS (b) CS combined with 10% aqueous TCLPL in 1N HCl.

Table 3
TCLPLE inhibitor: Nyquist plot electrochemical impedance characteristics

Concentration of the aqueous extract of TCLPL leaves (%v/v)	Nyquist plot		Impedance Log (z/ohm)	Phase angle (degree)
	R_t, Ω /cm^2	C_{dl} F/cm^2		
blank	6.72	1.1082×10^{-5}	0.845	33.0
10	22.52	3.7100×10^{-5}	1.359	49.0

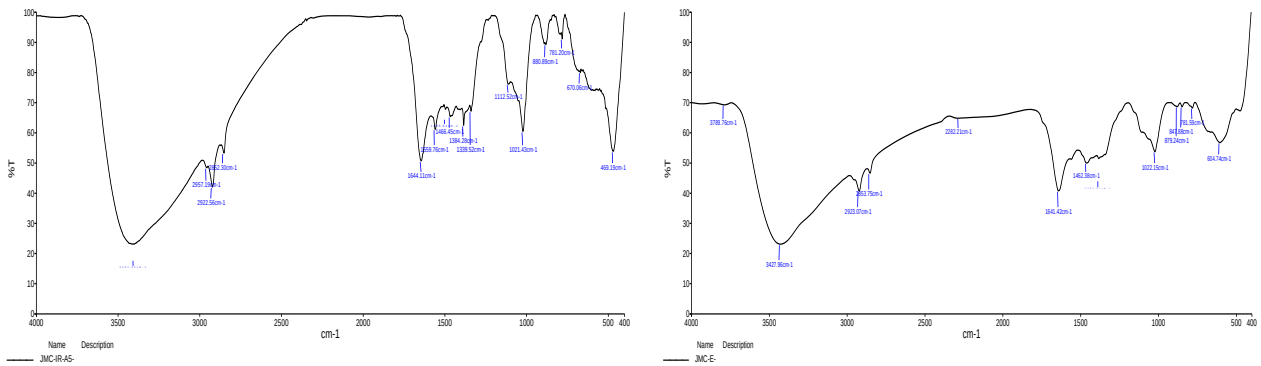

Fig. 5a: FTIR spectrum of aqueous extract of TCLPL
Fig. 5b: FTIR spectra of scratched CS sheet following immersion in 1N HCl with 10% TCLPL aqueous extract.

A change from 2923.07 to 2922.56 cm^{-1} is seen in the C-H group in the pure IR spectra of the TCL aqueous leaves extract and the protective layer that is produced over the CS surface. With the change from 1641.42 to 1644.11 cm^{-1} for the C=O group frequency, 604.74 cm^{-1} becomes 670.06 cm^{-1} and 1022.15 to 1021.43 cm^{-1} for the peak due to C-C stretching, the band is dominated by the Fe-complex 400–469 nanometers[19,31]. The presence of a protective layer on CS and the presence of almost all band peaks in TCLP leaf aqueous extract are very congruent, indicating that inhibitor molecule phytochemical components have adsorbed on the surface of CS.

SEM: The CS specimen is in 1N HCl with an inhibitor for three hours. After removing and drying the specimen, it is examined under a Scanning electron microscope. Images of freshly cut CS (control) in fig. 6a demonstrate its flat surface and the lack of any corrosion inhibitors that may have grown on it[26]. In fig. 6b, we can see that the CS surface has been corroded as a result of metal dissolving in 1N HCl. The heavily corroded section is shown by the rough CS surface. Figure 6c shows the CS surface submerged in 1N HCl with an inhibitor. The presence of an inhibitor (10% TCLPLE) reduces the extent of corrosion.

EDAX Analysis: Figure 7a displays the EDAX spectrum of CS, which includes the identifying peaks of many of the components that make up the CS sample. Figure 7b displays the EDAX spectrum of CS that has been submerged in 1N HCl; this spectrum reveals a reduction in the carbon constituent components. In addition, the presence of Cl^- shows that the CS was attacked by 1N HCl. Fig. 7c shows the EDAX spectrum of CS that has been submerged in 1N HCl and 10% water-based TCL plant-leaf extract.

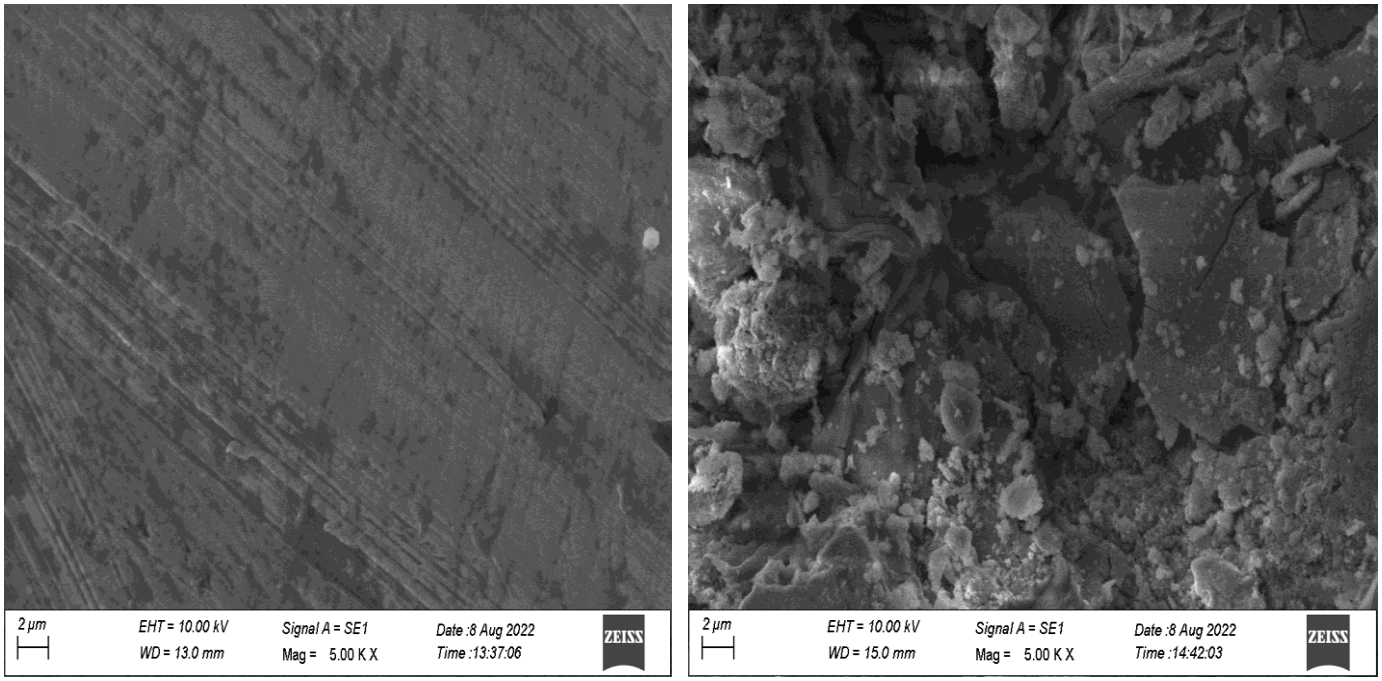

Fig. 6(a): SEM (control) Fig. 6(b): SEM (blank)

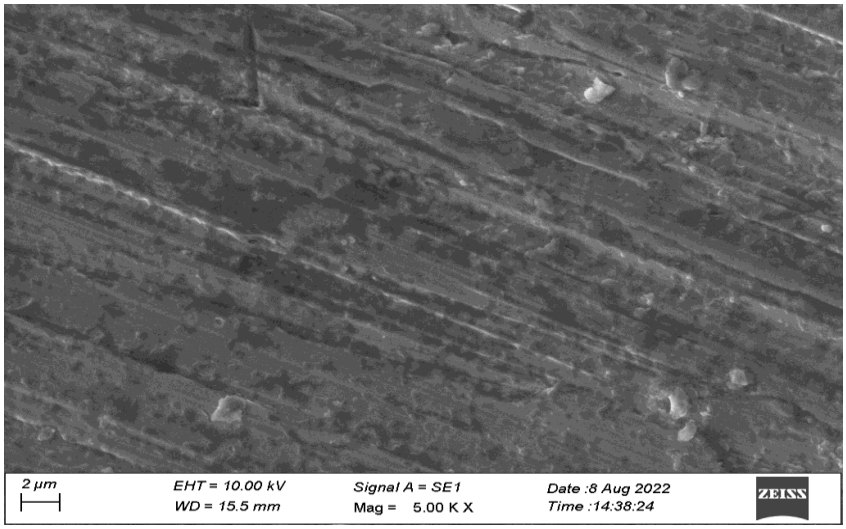

Fig. 6c: SEM picture of polished CS specimen in 1N HCl with 10% TCLPL aqueous extract.

Table 4
FTIR spectra analysis

IR bands of crude extract of TCL plant leaves	IR bands of defensive layer from CS surface	Frequency assignment to functional groups
3427.96	3401.42	-OH
2923.07	2922.56	C-H stretching
1641.42	1644.11	C=O stretching
1022.15	1021.43	C-C stretching
1462.38	1384.28	C-N
604.74	670.06	N-H
-	469.19	Y-Fe_20_3

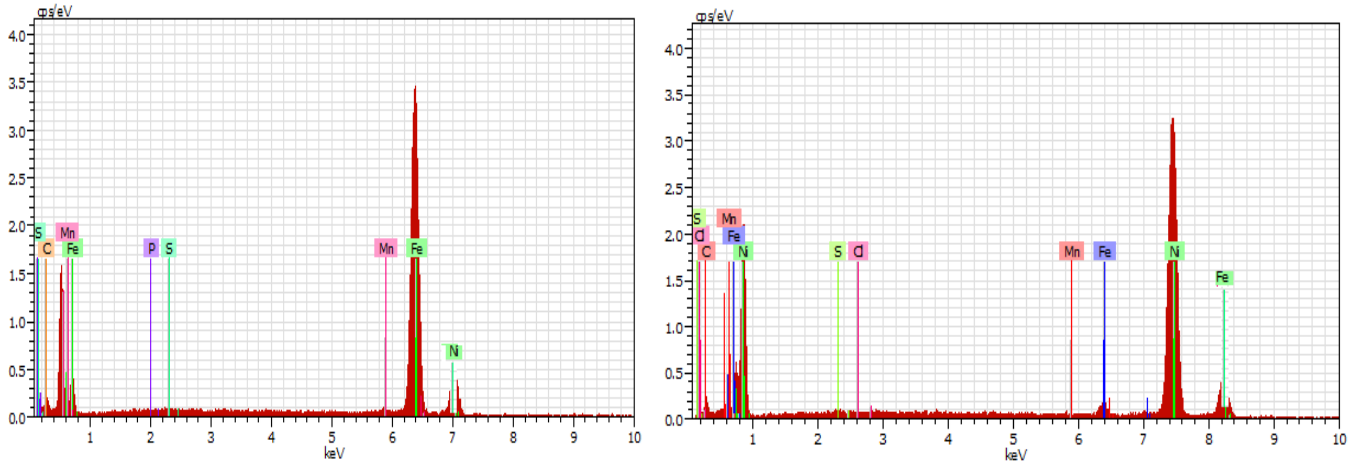

Fig. 7a: EDAX (control) Fig. 7b: EDAX (blank)

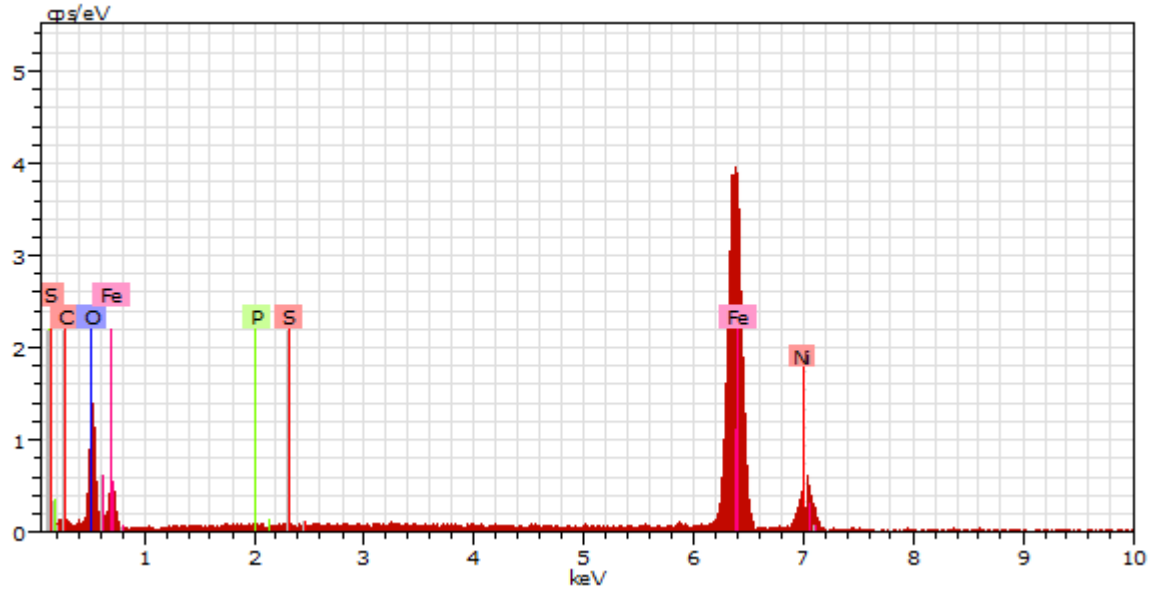

Fig. 7c: An EDAX picture of a finished piece of CS that was put in a solution of 1N HCl and 10% TCLPL water extract

It demonstrates that the CS signal's constituent parts have a higher intensity and the Cl^- signal's extra line characteristic has a lower one. The presence of the inhibitor is responsible for the emergence of the Fe signal and the increase of the O signal. The peaks caused by Fe and Ni are quite prominent in polished CS. The intensity of Fe is diminished for CS surfaces submerged in corrosive media. Corrosion products, including Fe_2O_3, are to blame for this. As a result of nickel being released during corrosion, the intensity of Ni is high. The inhibitor mechanism causes the Fe and Ni peaks to be less intense compared to polished CS because a protective coating is there.

The results demonstrate that CS has a surface coating of

atoms of Fe, S, C, P, Ni and O. This finding provides further evidence that CS has an inhibitory adsorption layer that prevents corrosion. These findings indicate that CS surfaces may adsorb oxygen, nitrogen and carbon atoms from 10% aqueous TCL plant leaf extract, leading to the development of a Fe^{2+}-TCL plant leaves complex[28,37].

Surface characterization of CS by AFM: The figures 8a, b and c show the polished CS surface (control sample), CS exposed to 1N HCl (blank sample) and CS surface treated with a corrosion inhibitor (10% aqueous extract of TCLPL) submerged in 1N HCl. These pictures show the three-dimensional (3D) morphologies and cross-sectional profiles obtained using AFM[34].

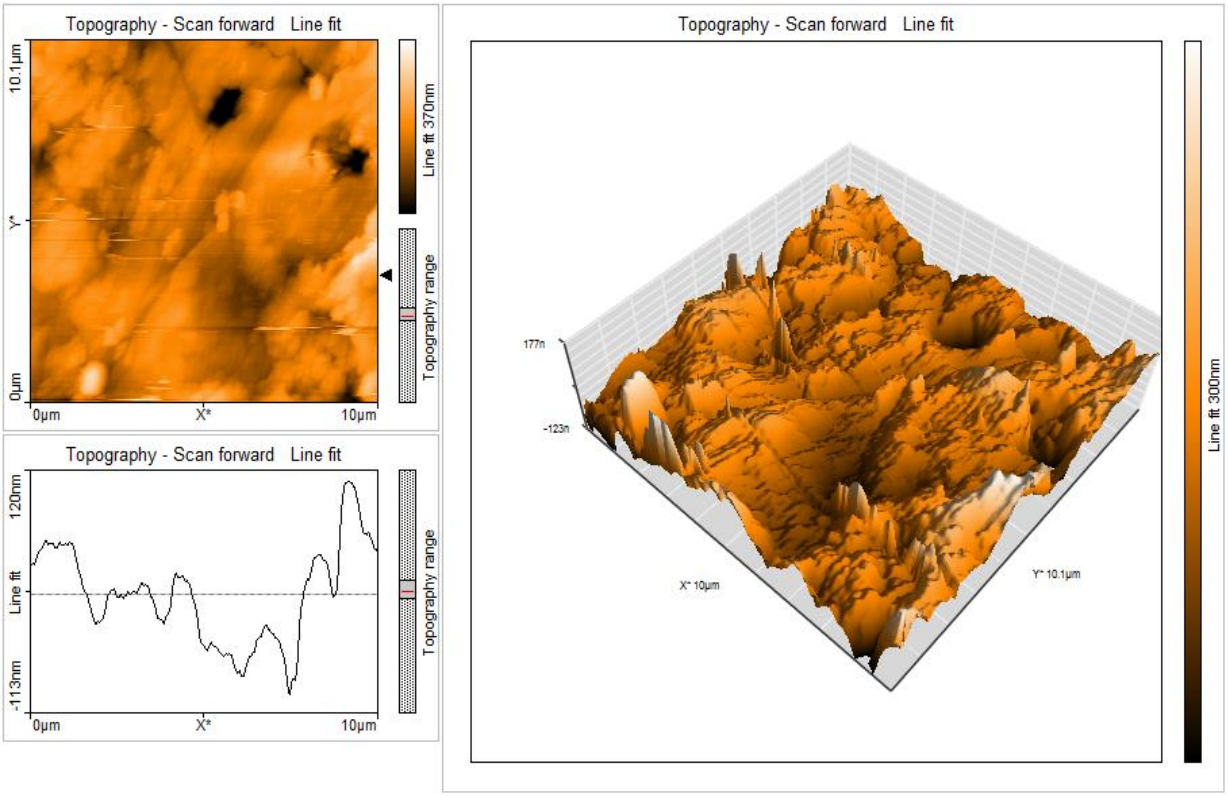

Fig. 8a: AFM (control)

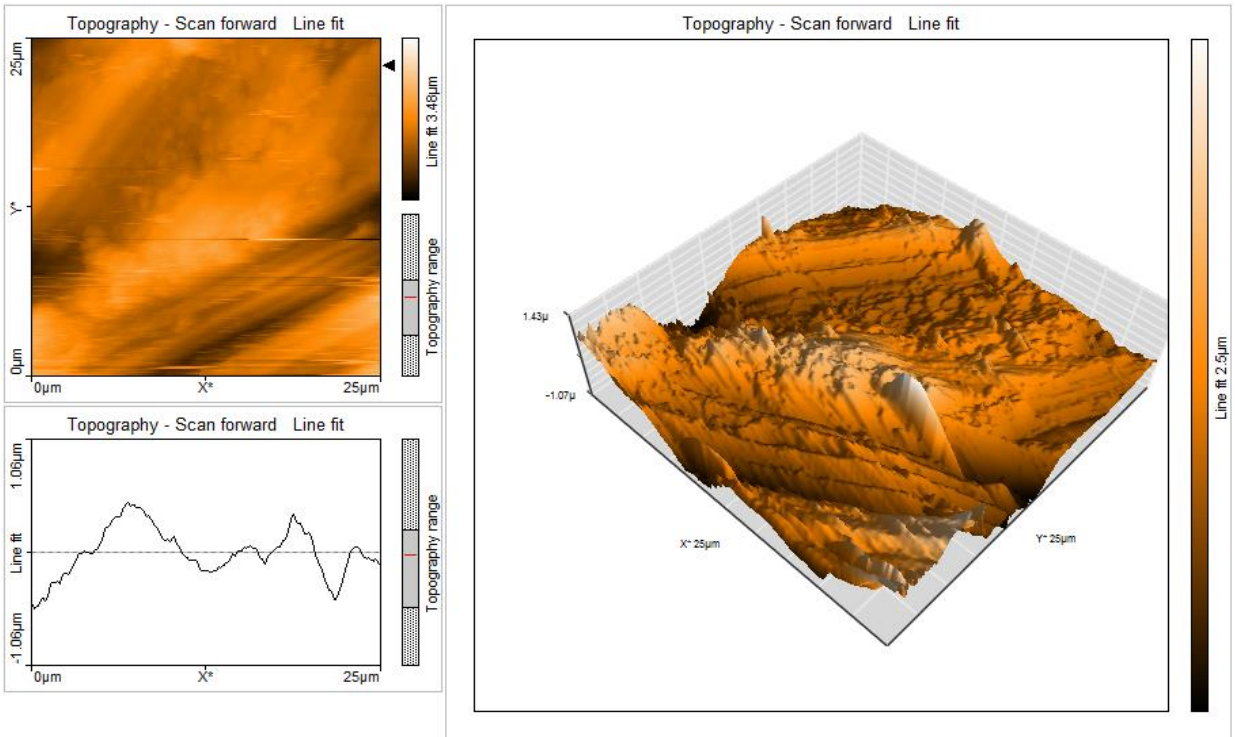

Fig. 8b: AFM (blank)

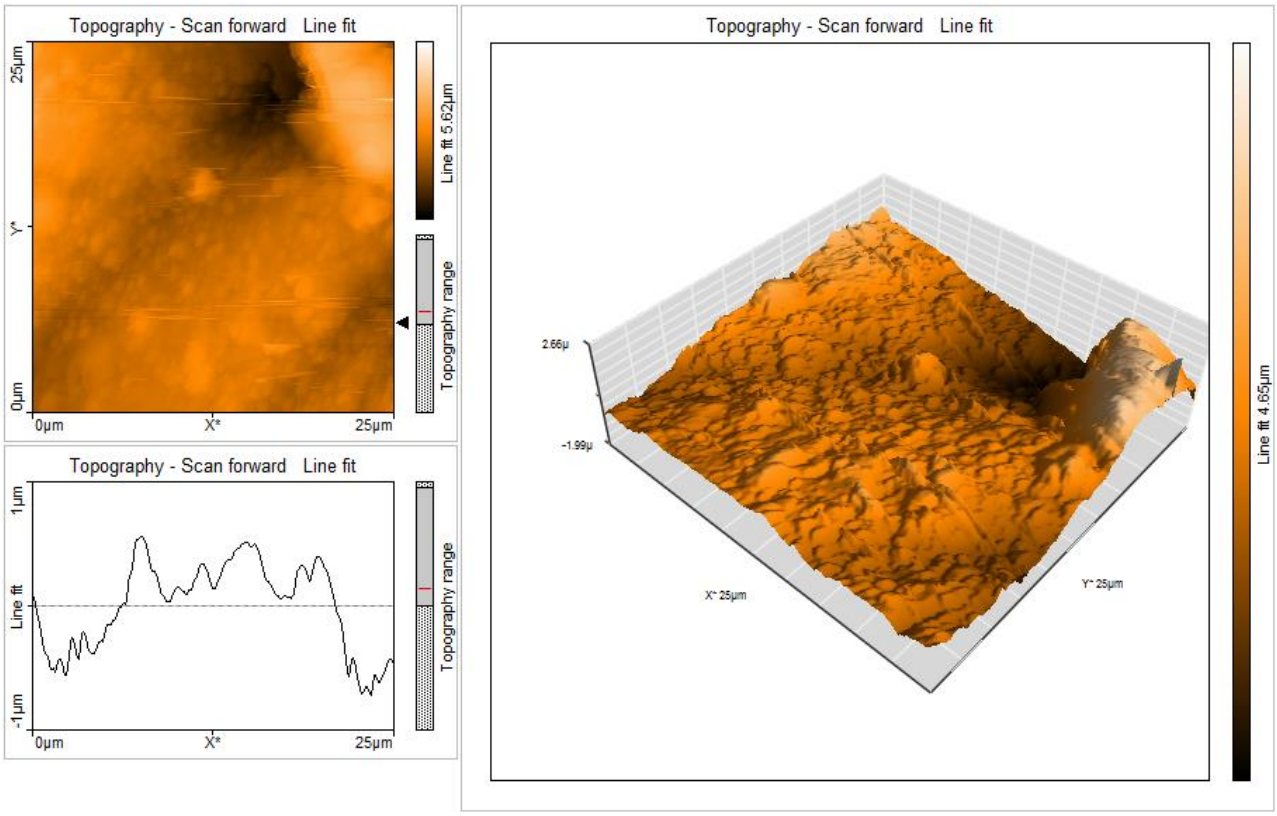

Fig. 8c: AFM – CS specimen

Table 5
AFM data

System	Surface roughness (nm)			Line roughness (nm)		
	Average roughness (S_a)	**Root mean square roughness (S_q)**	**Maximum peak to valley (P-V) height (S_y)**	**Average roughness (R_a)**	**Root mean square roughness (R_q)**	**Maximum peak to valley (P-V) height (R_y)**
Polished carbon steel	31.44	42.38	495.40	33.38	48.774	229.50
CS + 1N HCl	273.72	348.79	3334.00	342.25	403.34	1611.94
CS in 1N HCl with 10 % of aqueous extract of TCLP leaves	254.48	321.07	1415.3	446.68	614.24	506.40

The polished CS has an RMS roughness of 42.38 nm as shown in table 5. An average of 31.44 nanometers is the roughness of the surface. The maximum height variation amplitude is 495.40 nm. According to the data in table 5, CS has a higher root mean square (RMS) roughness when subjected to 1N HCl, a corrosive medium, compared to polished CS. The corrosion has caused this. The average roughness and maximum peak-to-valley height are similarly affected[19]. Submerged metal in an inhibitor system has a lower RMS roughness than metal in a corrosive medium. When considering maximal peak-to-valley height and average roughness, the situation is quite similar. A dense coating of nanofilm covers the surface of the metal[20]. The information suggests that a nanoscale layer is formed on the metal's surface. When this compound is applied to the metal, it becomes resistant to corrosion.

Conclusion

The corrosion inhibitor system, which comprises of 10% TCLPLE, obtained a maximum inhibition effectiveness of 86.63% in controlling the corrosion of CS in 1N HCl, based on the mass-loss technique. Adsorption of inhibitor chemicals from TCL plant leaves extract onto CS surfaces increases inhibition efficiency and decreases corrosion rate. CS develops a protective layer, or "blanket effect," according to electrochemical impedance tests. This results in an increase in charge transfer resistance and a reduction in double layer capacitance when an inhibitor system is present. The potentiodynamic polarisation experiment

demonstrates how the formulation works as a mixed type inhibitor by regulating the anodic and cathodic processes.

A mixture of Fe^{2+} and an inhibitor makes up the protective coating on the surface of CS, according to the FTIR spectra. With and without an aqueous extract of TCL plant leaves inhibitor, the SEM analysis of the CS surface coating's composition and properties was performed. Using EDAX spectra, both before and after the polished CS surface was exposed to the inhibitor solution, the component composition was studied. AFM was used to examine the CS surface roughness with and without the TCLPLE inhibitor.

Acknowledgement

The authors would like to convey their deepest appreciation to the Principal and the College Management Committee of Jamal Mohamed College (Autonomous), Tiruchirappalli, Tamil Nadu, India. Thanks also go to the instrumental resources provided by the DST-FIST.

References

1. Adebooye O.C., Phyto-constituents and anti-oxidant activity of the pulp of snake tomato (Trichosanthes cucumerina L.), *African Journal of Traditional, Complementary and Alternative Medicines*, **5(2),** 173-179 **(2008)**

2. Al Kiey S.A. and Hasanin M.S., Green and sustainable chitosan–gum Arabic nanocomposites as efficient anticorrosive coatings for mild steel in saline media, *Scientific Reports*, **12(1)**, 1-16 **(2022)**

3. Angst U.M., Challenges and opportunities in corrosion of steel in concrete, *Materials and Structures*, **51(1)**, 1-20 **(2018)**

4. Anuradha P. and Bhide S.V., An isolectin complex from *Trichosanthes anguina* seeds, *Phytochemistry*, **52(5)**, 751-758 **(1999)**

5. Asiya S.I. and Pal K., Bio-Inspired Self-Assembly Green Nanomaterials for Multifunctional Applications, Green Nanomaterials, Apple Academic Press, 1-28 **(2022)**

6. Bahlakeh G., Ramezanzadeh B., Dehghani A. and Ramezanzadeh M., Novel cost-effective and high-performance green inhibitor based on aqueous Peganum harmala seed extract for mild steel corrosion in HCl solution: Detailed experimental and electronic/atomic level computational explorations, *Journal of Molecular Liquids*, **283**, 174-195 **(2019)**

7. Basiony N.E., Elgendy A., Nady H., Migahed M.A. and Zaki E.G., Adsorption characteristics and inhibition effect of two schiff base compounds on corrosion of mild steel in 0.5 M HCl solution: experimental, DFT studies and Monte Carlo simulation, *RSC Advances*, **9(19)**, 10473-10485 **(2019)**

8. Brixi N.K., Sail L. and Bezzar A., Application of ascorbic acid as green corrosion inhibitor of reinforced steel in concrete pore solutions contaminated with chlorides, *Journal of Adhesion Science and Technology*, **36(11)**, 1176-1199 **(2022)**

9. Chow L.P., Chou M.H., Ho C.Y., Chuang C.C., Pan F.M., Wu S.H. and Lin J.Y., Purification, characterization and molecular cloning of trichoanguin, a novel type I ribosome-inactivating protein from the seeds of *Trichosanthes anguina*, *Biochemical Journal*, **338(1)**, 211-219 **(1999)**

10. Chong A.L., Mardel J.I., MacFarlane D.R., Forsyth M. and Somers A.E., Synergistic corrosion inhibition of mild steel in aqueous chloride solutions by an imidazolinium carboxylate salt, *ACS Sustainable Chemistry & Engineering*, **4(3)**, 1746-1755 **(2016)**

11. Chaudhary S. and Tak R.K., Natural corrosion inhibition and adsorption characteristics of tribulusterrestris plant extract on aluminium in hydrochloric acid environment, *Biointerface Res. Appl. Chem*, **12(2)**, 2603-2617 **(2022)**

12. Datta S.K., Fatty acid composition in developing seeds of *Trichosanthes cucumerina* L., *Biological Memoirs*, **13(1)**, 69-72 **(1987)**

13. Dehghani A., Bahlakeh G. and Ramezanzadeh B., Green Eucalyptus leaf extract: a potent source of bio-active corrosion inhibitors for mild steel, *Bioelectrochemistry*, **130**, 107339 **(2019)**

14. El Bribri A., Tabyaoui M., Tabyaoui B., El Attari H. and Bentiss F., The use of Euphorbia falcata extract as eco-friendly corrosion inhibitor of CS in hydrochloric acid solution, *Materials Chemistry and Physics*, **141(1)**, 240-247 **(2013)**

15. Fattah-alhosseini A. and Chaharmahali R., Enhancing corrosion and wear performance of PEO coatings on Mg alloys using graphene and graphene oxide additions: A review, *Flat Chem*, **27**, 100241 **(2021)**

16. Ghaderi S., Haddadi S.A., Davoodi S. and Arjmand M., Application of sustainable saffron purple petals as an eco-friendly green additive for drilling fluids: A rheological, filtration, morphological and corrosion inhibition study, *Journal of Molecular Liquids*, **315**, 113707 **(2020)**

17. Hajjaji F.E., Salim R., Ech-chihbi E., Titi A., Messali M., Kaya S. and Taleb M., New imidazolium ionic liquids as ecofriendly corrosion inhibitors for mild steel in hydrochloric acid (1 M): Experimental and theoretical approach, *Journal of the Taiwan Institute of Chemical Engineers*, **123**, 346-362 **(2021)**

18. Joycee S.C., Vidya T., Rattihka S.A., Prabha B.S., Dorothy R., Sasilatha T. and Rajendran S., Corrosion resistance of mild steel in simulated concrete pore solution before and after a paint coating, *International Journal of Corrosion and Scale Inhibition*, **10(3)**, 1323-1335 **(2021)**

19. Karthikeyan S., Abuthahir S.S.S., Begum A.S., Rajendran S. and Al-Hashem A., Inhibition of mild steel corrosion in 0.5 M sulfuric acid by an aqueous extract of leaves of *Tectona grandis L.* plant, *Int. J. Corros. Scale Inhib*, **10(4)**, 1531-1546 **(2021)**

20. Karthikeyan S., Syed Abuthahir S.S., Samsath Begum A. and Vijaya K., Corrosion Inhibition of Mild Steel in 0.5 M H_2SO_4 Solution by Plant Extract of *Annona squamosal*, *Asian Journal of Chemistry*, **33(9)**, 2219-2228 **(2021)**

21. Mourya P., Banerjee S. and Singh M.M., Corrosion inhibition of mild steel in acidic solution by *Tagetes erecta* (Marigold flower) extract as a green inhibitor, *Corrosion Science*, **85**, 352-363 **(2014)**

22. Madhubala M. and Santhi G., Phytochemical and GC-MS

analysis on leaves of selected medicinal plants in Boraginaceae family *Cordia dichotoma L*, *Pramana Res. J*, **9**, 2249-2276 **(2019)**

23. Neraliya S. and Srivastava U.S., Juvenomimetic activity in some Indian angiosperm plants, *J Med Aromot Plant Sci*, **19**, 677-81 **(1997)**

24. Naderi R., Bautista A., Velasco F., Soleimani M. and Pourfath M., Use of licorice plant extract for controlling corrosion of steel rebar in chloride-polluted concrete pore solution, *Journal of Molecular Liquids*, **346**, 117856 **(2022)**

25. Nagalakshmi R., Sathiyabama J., BashaI. A. and Johnmary S., Invitro Corrosion studies on Nickel Titanium Super elastic alloy in synthetic urine in presence of D-Glucose, *International Journal of Materials Science*, **12(2)**, 51-59 **(2017)**

26. Naderi R., Bautista A., Velasco F., Soleimani M. and Pourfath M., Green corrosion inhibition for CS reinforcement in chloride-polluted simulated concrete pore solution using *Urtica Dioica* extract, *Journal of Building Engineering*, **58**, 105055 **(2022)**

27. Obot I.B., Gasem Z.M. and Umoren S.A., Molecular level understanding of the mechanism of aloes leaves extract inhibition of low CS corrosion: a DFT approach, *Int. J. Electrochem. Sci*, **9**, 510-522 **(2014)**

28. Pandiarajan M., Prabhakar P. and Rajendran S., Corrosion resistance of mild steel in simulated concrete pore solution, *Chem Sci Trans*, **2(2)**, 605-613 **(2013)**

29. Rajendran S., Agasta M., Devi R.B., Devi B.S., Rajam K. and Jeyasundari J., Corrosion inhibition by an aqueous extract of Henna leaves (LawsoniaInermis L), *Zast. Mater*, **50**,77–84 **(2009)**

30. Ramezanzadeh M., Bahlakeh G., Sanaei Z. and Ramezanzadeh B., Corrosion inhibition of mild steel in 1 M HCl solution by ethanolic extract of eco-friendly Mangifera indica (mango) leaves: electrochemical, molecular dynamics, Monte Carlo and ab initio study, *Applied Surface Science*, **463**, 1058-1077 **(2019)**

31. Raja T. and Syed Abuthahir S.S., Electrochemical behaviour of CS in sodium chloride solution by using thiophenol derivative inhibitor, Materials Today Proceedings, **69**, 1501-1508 **(2022)**

32. Shanmugapriya S., Rajendran S., Prabhakar P., Rathish R.J., Mary A.C.C. and Devi R., Influence of extract of Curcumalonga on the corrosion resistance of mild steel immersed in Simulated Concrete Pore Solution prepared in well water, *Int. J. Nano. Corr. Sci. Engg*., **2(5)**, 70-83 **(2015)**

33. Suriyaprabha A., Sathiyabama J., Rajendran S., Rathish R.J. and Umasankareswari T., Influence of chloride ion in corrosion inhibition of mild steel in simulated concrete pore solution-an overview, *Int J Nano Corr Sci and Engg*, **4(2)**, 41-81 **(2017)**

34. Vijayakumar P., Valarselvan S. and Syed Abuthahir S.S., Corrosion Resistance, Electrochemical and surface morphology studies of mild steel in a sulfuric acid medium by using dibutyl sulphide, *Portugaliae Electrochimica Acta*, **41**, 1-15 **(2023)**

35. Zakeri A., Bahmani E. and Aghdam A.S.R., Plant extracts as sustainable and green corrosion inhibitors for protection of ferrous metals in corrosive media: A mini review, *Corrosion Communications*, **5**, 25-38 **(2022)**

36. Zhu M., He Z., Guo L., Zhang R., Anadebe V.C., Obot I.B. and Zheng X., Corrosion inhibition of eco-friendly nitrogen-doped carbon dots for CS in acidic media: Performance and mechanism investigation, *Journal of Molecular Liquids*, **342**, 117583 **(2021)**

37. Zhang Z., Ba H. and Wu Z., Sustainable corrosion inhibitor for steel in simulated concrete pore solution by maize gluten meal extract: Electrochemical and adsorption behavior studies, *Construction and Building Materials*, **227**, 117080 **(2019)**.

(Received 24th June 2024, revised 24th October 2024, accepted 14th November 2024)